Article

Cancer Cell

FOXK2 Elicits Massive Transcription Repression and Suppresses the Hypoxic Response and Breast Cancer Carcinogenesis

Graphical Abstract

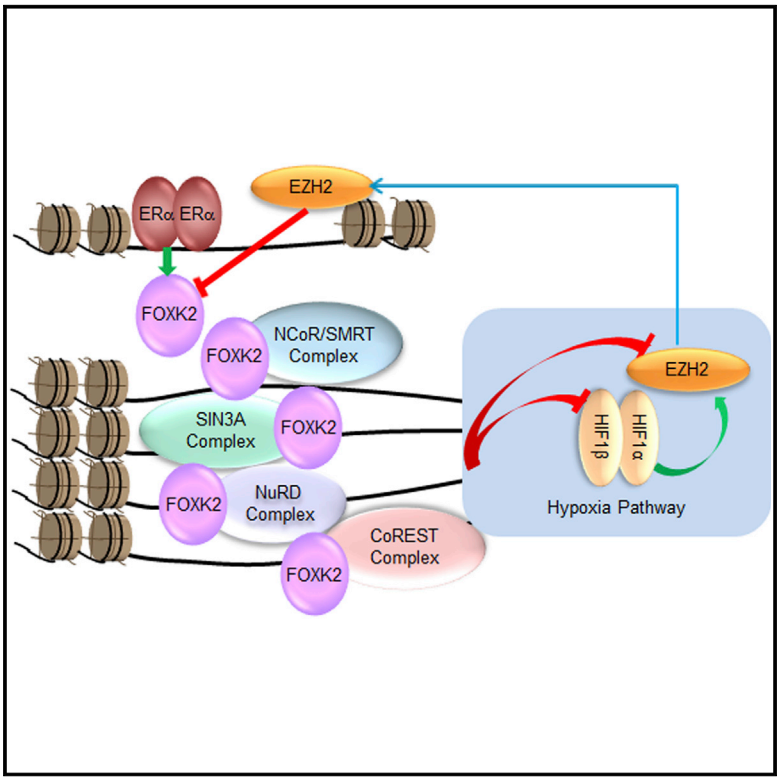

Authors

Lin Shan, Xing Zhou, Xinhua Liu, ..., Lei Shi, Yan Wang, Yongfeng Shang

Correspondence

yshang@hsc.pku.edu.cn

In Brief

Shan et al. show that FOXK2 interacts with multiple corepressor complexes to repress the expression of a cohort of genes including HIF1β and EZH2. They show that an ERα-FOXK2-HIF1β/EZH2 axis is critically involved in breast cancer progression and that low FOXK2 expression correlates with poor prognosis.

Highlights

- FOXK2 is a transcription repressor
- FOXK2 is physically associated with multiple corepressor complexes
- FOXK2 and its associated corepressor complexes target the hypoxia pathway
- FOXK2 suppresses the growth and metastasis of breast cancer

Accession Numbers

GSE84241

Shan et al., 2016, Cancer Cell *30*, 708–722
November 14, 2016
http://dx.doi.org/10.1016/j.ccell.2016.09.010

CellPress

CellPress

Cancer Cell
Article

FOXK2 Elicits Massive Transcription Repression and Suppresses the Hypoxic Response and Breast Cancer Carcinogenesis

Lin Shan,[1] Xing Zhou,[1] Xinhua Liu,[1] Yue Wang,[1] Dongxue Su,[1] Yongqiang Hou,[1] Na Yu,[1] Chao Yang,[1] Beibei Liu,[1] Jie Gao,[1] Yang Duan,[1] Jianguo Yang,[2] Wanjin Li,[2] Jing Liang,[2] Luyang Sun,[2] Kexin Chen,[3] Chenghao Xuan,[1] Lei Shi,[1] Yan Wang,[1] and Yongfeng Shang[1,2,4,*]

[1]Department of Biochemistry and Molecular Biology, 2011 Collaborative Innovation Center of Tianjin for Medical Epigenetics, Tianjin Key Laboratory of Medical Epigenetics, School of Basic Medical Sciences, Tianjin Medical University, 22 Qixiangtai Road, Tianjin 300070, China
[2]Key Laboratory of Carcinogenesis and Translational Research (Ministry of Education), Department of Biochemistry and Molecular Biology, School of Basic Medical Sciences, Peking University Health Science Center, Beijing 100191, China
[3]Department of Epidemiology and Biostatistics, Tianjin Medical University Cancer Institute and Hospital, Tianjin 300060, China
[4]Lead Contact
*Correspondence: yshang@hsc.pku.edu.cn
http://dx.doi.org/10.1016/j.ccell.2016.09.010

SUMMARY

Although clinically associated with severe developmental defects, the biological function of FOXK2 remains poorly explored. Here we report that FOXK2 interacts with transcription corepressor complexes NCoR/SMRT, SIN3A, NuRD, and REST/CoREST to repress a cohort of genes including *HIF1β* and *EZH2* and to regulate several signaling pathways including the hypoxic response. We show that FOXK2 inhibits the proliferation and invasion of breast cancer cells and suppresses the growth and metastasis of breast cancer. Interestingly, FOXK2 is transactivated by ERα and transrepressed via reciprocal successive feedback by HIF1β/EZH2. Significantly, the expression of FOXK2 is progressively lost during breast cancer progression, and low FOXK2 expression is strongly correlated with higher histologic grades, positive lymph nodes, and ERα^{-}/PR^{-}/HER2^{-} status, all indicators of poor prognosis.

INTRODUCTION

Despite recent advances in the understanding of the forkhead box (FOX) family of transcription factors, the biological functions of the majority of the forkhead family of proteins including FOXK1 and FOXK2 remain to be explored.

It is reported that FOXK1 and FOXK2 transcriptionally regulate starvation-induced atrophy and autophagy programs through recruitment of the SIN3A complex (Bowman et al., 2014). In addition to the SIN3A complex, FOXK2 also interacts with BRCA1-associated protein 1 (BAP1) deubiquitinase in its transcriptional regulatory activity (Ji et al., 2014; Okino et al., 2015). Interestingly, it is also reported that FOXK2 functions non-genomically by translocating Dishevelled protein (DVL) into the nucleus to positively regulate Wnt signaling (Wang et al., 2015) or through acting as a scaffold protein to regulate ubiquitin-mediated degradation of estrogen receptor (ERα) (Liu et al., 2015b). Remarkably, partial tetrasomy of chromosome 17q25.3 was detected in a 10-year-old girl with severe intellectual disability, West syndrome, Dandy-Walker malformation, and syndactyly; the breakpoint at 17q25.3 for the chromosome rearrangement was located within the FOXK2 gene (Hackmann et al., 2013), suggesting a pivotal role for FOXK2 in development. As accumulating evidence indicates that a number of transcription factors that are required for normal development are also involved in tumor development, a role for FOXK2 in tumorigenesis is expected. However, little is known about the role of FOXK2 in tumor development and progression.

Significance

Our experiments show that lost expression of FOXK2 during breast cancer progression is linked to elevated expression of EZH2, an eminent feature of aggressive breast cancer. We find that, indeed, the expression of FOXK2 is inversely correlated with that of EZH2 and HIF1β in breast carcinomas. Our study reveals that FOXK2 is involved in transcription repression, providing a molecular basis for the understanding of the mechanistic action of FOXK2. Our results indicate that the ERα-FOXK2-HIF1β/EZH2 axis is critically implemented in breast cancer progression, supporting the pursuit of these molecules as therapeutic targets for breast cancer intervention.

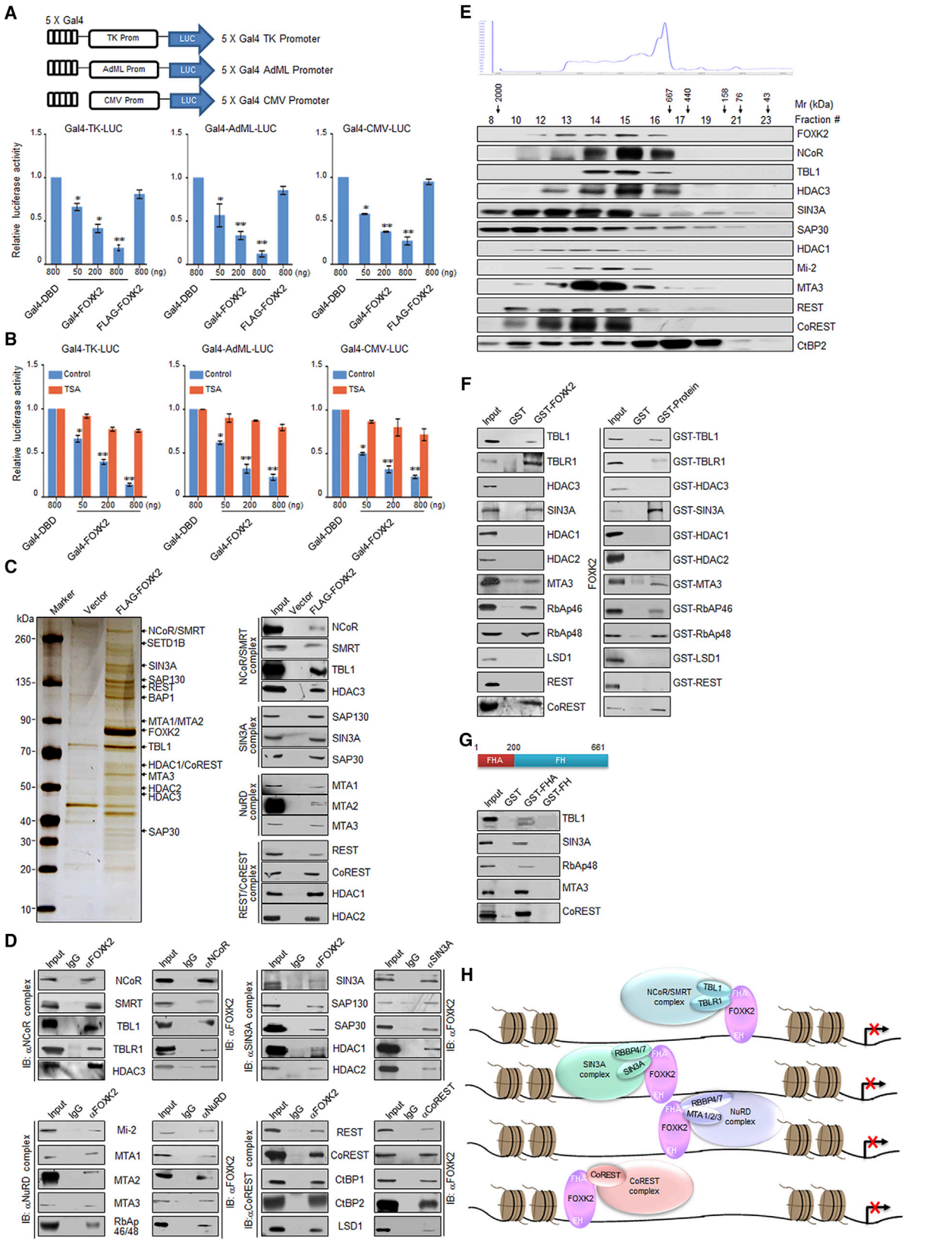

(legend on next page)

The majority of cellular activity is determined by tightly controlled transcription programs that enable or disable gene expression. The on or off control of gene expression involves numerous transcription factors and is assisted by a cascade of co-activators or corepressors. These cofactors act in a combinatorial manner and coordinated fashion to influence the chromatin environment, thereby regulating the accessibility of the transcription machinery to chromatin. Specifically, transcription repression involves the recruitment of distinct corepressor complexes including NCoR/SMRT, SIN3A, NuRD, and REST/CoREST, all contain chromatin-modifying activities such as histone deacetylase (HDAC). These corepressor complexes are recruited by a broad array of transcription factors and participate in a variety of cellular activities. Consequently, dysfunction of these corepressor complexes has been implicated in various pathological states including malignant transformation (Dannenberg et al., 2005; Lai and Wade, 2011; Westbrook et al., 2005; Wong et al., 2014).

In the current study, we investigated the transcriptional activity, genomic targets, cellular function, and regulation of FOXK2, and explored the role of FOXK2 in breast carcinogenesis.

RESULTS

FOXK2 Is a Transcription Repressor and Physically Associated with Multiple Transcription Corepressor Complexes

In order to explore the cellular activity of FOXK2, we first investigated the transcriptional activity of this transcription factor. For this purpose, full-length FOXK2 was fused to the C terminus of the Gal4 DNA-binding domain (Gal4-FOXK2) and the transcriptional activity of the fused construct was tested in HeLa cells. We used three different Gal4-driven luciferase reporter systems that all contain five copies of the Gal4 binding sequence but differ in basal promoter elements. The results showed that FOXK2 elicited a robust repression of the reporter activity in a dose-dependent fashion in all of the reporter systems (Figure 1A). Meanwhile, overexpression of FLAG-FOXK2 had no effect on the activity of Gal4-driven reporters (Figure 1A), suggesting that FOXK2 must be physically associated with DNA to exert its transcription repression activity.

To determine if HDAC activity is required for FOXK2-mediated gene repression, we measured the reporter activity in HeLa cells under the treatment of trichostatin A (TSA), a specific HDAC inhibitor. The results indicate that TSA treatment was able to almost completely alleviate the repression of the reporter activity by FOXK2 (Figure 1B), suggesting that FOXK2-mediated repression was associated with an HDAC activity.

In order to gain a mechanistic insight into the transcription repression function of FOXK2, we employed affinity purification and mass spectrometry to interrogate the FOXK2 interactome in vivo. In these experiments, FLAG-FOXK2 was stably expressed in human breast adenocarcinoma MCF-7 cells. Cellular extracts were subjected to affinity purification using an anti-FLAG affinity column and the bound proteins were analyzed by mass spectrometry. The results showed that FOXK2 was co-purified with a list of proteins, including NCoR, SMRT, TBL1, and HDAC3, all components of the NCoR/SMRT complexes; SIN3A, SAP130, SAP30, HDCA1, and HDCA2, all constituents of the SIN3A complex; MTA1, MTA2, and MTA3, subunits of the NuRD complex; and REST and CoREST, subunits of the REST/CoREST complex (Figure 1C, left). Additional proteins including BAP1 and SETD1B were also detected in the FOXK2-containing complex (Figure 1C, left). The presence of these proteins in the FOXK2-associated protein complex was confirmed by western blotting of the column eluates (Figure 1C, right). These results indicate that FOXK2 is associated with multiple transcription corepressor complexes in vivo. The detailed results of the mass spectrometric analysis are provided in Table S1.

To confirm the in vivo interaction between FOXK2 and the corepressor complexes, total proteins from MCF-7 cells were extracted and co-immunoprecipitation was performed with antibodies detecting the endogenous proteins. Immunoprecipitation (IP) with antibodies against FOXK2 followed by immunoblotting (IB) with antibodies against the components of the corepressor complexes demonstrated that these corepressor components were efficiently co-immunoprecipitated with FOXK2 (Figure 1D). Reciprocally, IP with antibodies against representative components of the NCoR/SMRT, SIN3A, NuRD, and REST/CoREST complexes and IB with antibodies against FOXK2 also showed that FOXK2 was efficiently co-immunoprecipitated with the components of these corepressor complexes (Figure 1D). The associations between FOXK2 and these corepressor complexes were also detected in HEK293T cells (Figure S1A).

Figure 1. FOXK2 Is a Transcription Repressor and Interacts with Multiple Transcription Corepressor Complexes

(A) The schematic diagrams of the Gal4-luciferase reporter constructs. For reporter assays, HeLa cells were transfected with Gal4-DBD, different amounts of Gal4-FOXK2 or FLAG-FOXK2, together with the indicated Gal4-luciferase reporter for luciferase activity assay. *$p < 0.05$, **$p < 0.01$.

(B) HeLa cells were transfected with the indicated plasmids and treated with trichostatin A (TSA) for luciferase activity assay. Each bar represents the mean ± SD for triplicate experiments. *$p < 0.05$, **$p < 0.01$.

(C) Immunopurification and mass spectrometry analysis of FOXK2-associated proteins. Cellular extracts from FLAG-FOXK2-expressing MCF-7 cells were subjected to affinity purification with anti-FLAG affinity columns and eluted with FLAG peptide. The elutes were resolved by SDS-PAGE and silver-stained (left). The protein bands were retrieved and analyzed by mass spectrometry. Column-bound proteins were analyzed by western blotting using antibodies against the indicated proteins (right).

(D) Co-immunoprecipitation assays in MCF-7 cells with anti-FOXK2 followed by immunoblotting (IB) with antibodies against the indicated proteins, or with antibodies against the indicated proteins followed by IB with anti-FOXK2.

(E) Fast protein liquid chromatography experiments in MCF-7 cells. Chromatographic elution profiles and IB of the chromatographic fractions are shown. Equal volume from each fraction was analyzed and the elution positions of calibration proteins with known molecular masses (kDa) are indicated.

(F) GST pull-down assays with bacterially expressed GST-fused proteins and in vitro transcribed/translated proteins as indicated.

(G) GST pull-down assays with GST-fused FOXK2 forkhead (FH) or FH-associated (FHA) domain and in vitro transcribed/translated proteins as indicated.

(H) Schematic representation of the interaction between FOXK2 and the corepressor complexes. FOXK2 interacts with the NCoR/SMRT, SIN3A, NuRD, and REST/CoREST complexes through the indicated subunits to repress the expression of different sets of genes.

See also Table S1 and Figure S1.

To investigate whether the physical association of FOXK2 with multiple transcription corepressor complexes reflects a capability of FOXK2 to interact with all of these protein complexes simultaneously or that of FOXK2 to interact with different corepressor complexes under different cellular environments, MCF-7 cells expressing FLAG-FOXK2 were synchronized by serum deprivation for 24 hr. After 6 hr of nutrient replenishment, cellular extracts were prepared, and affinity purification and mass spectrometry were performed again. We detected the physical association of FOXK2 with all of the major transcription repression complexes in synchronized MCF-7 cells (Figure S1B), favoring an argument that FOXK2 interacts with the multiple corepressor complexes simultaneously in vivo.

Fast protein liquid chromatography experiments were then performed with nuclear extracts with Superose 6 columns and a high salt extraction and size-exclusion approach. Native FOXK2 from MCF-7 cells was eluted with an apparent molecular mass much greater than that of the monomeric protein; FOXK2 immunoreactivity was detected in chromatographic fractions from the Superose 6 column with a relatively symmetrical peak centered between ~669 and ~2000 kDa. Significantly, overlapping of the elution patterns between FOXK2 and the components of the corepressor complexes was detected in corresponding fractions (Figure 1E), further supporting the idea that FOXK2 is associated with the multiple corepressor complexes in vivo.

We next performed glutathione S-transferase (GST) pull-down assays using GST-fused FOXK2 and in vitro transcribed/translated components of the corepressor complexes. These experiments indicate that FOXK2 was capable of interacting with TBL1 and TBLR1 (NCoR/SMRT complexes), SIN3A (SIN3A complex), RbAp46, RbAp48, and MTA3 (NuRD complex), and CoREST (REST/CoREST complex), but not with the other components that we tested (Figure 1F, left). Reciprocally, GST pull-down experiments with GST-fused components of the corepressor complexes and in vitro transcribed/translated FOXK2 yielded similar results (Figure 1F, right).

FOXK2 contains two distinct structural domains: the C-terminal forkhead (FH) domain, also known as winged helix, and the N-terminal FH-associated (FHA) domain, a phosphopeptide recognition motif found in many regulatory proteins. GST pull-down assays with GST-fused FHA domain (amino acids [aa] 1–200) or FH domain (aa 201–661) and in vitro transcribed/translated TBL1, SIN3A, RbAp48, MTA3, and CoREST showed that the FHA domain is responsible for the interaction of FOXK2 with these proteins (Figure 1G). Together, these experiments not only revealed the molecular detail involved in the interaction of FOXK2 with the multiple corepressor complexes (Figure 1H), but also provided additional support to the physical association between FOXK2 and these corepressor complexes in vivo.

Genome-wide Identification of Transcriptional Targets for FOXK2 and Its Associated Corepressor Complexes

To understand the biological significance of the physical interaction between transcription repressor FOXK2 and the multiple corepressor complexes, we next analyzed the genome-wide transcriptional targets of FOXK2. To this end, chromatin immunoprecipitation (ChIP)-based deep sequencing (ChIP-seq) was performed in MCF-7 cells first using antibodies against FOXK2. Following ChIP, FOXK2-associated DNAs were amplified using nonbiased conditions, labeled, and sequenced via HiSeq 2000. With Model-based Analysis for ChIP-seq version 14 (MACS14) and a p value cutoff of 10^{-5}, we identified 11,717 FOXK2-specific binding peaks. The detailed results from the ChIP-seq experiments are deposited in GEO (GSE84241) and summarized in Table S2, and the representative ChIP-seq peak data are shown in Figure 2A (upper). The DNA sequences associated with these peaks were then cross-analyzed with publicly available ChIP-seq datasets for TBL1 (GSM865743), SIN3A (GSM1010862), REST (GSM1010891), and with our previously published ChIP-seq data for MTA3 (GSM1642517) for overlapping DNA sequences/gene promoters to represent the co-targets of the FOXK2/NCoR/SMRT complex, the FOXK2/SIN3A complex, the FOXK2/REST/CoREST complex, and the FOXK2/NuRD complex, respectively (Figure 2A, lower). These analyses identified a total of 1,311 promoters targeted by FOXK2 and TBL1, 2,079 promoters regulated by FOXK2 and SIN3A, 1,503 promoters targeted by FOXK2 and MTA3, and 449 promoters regulated by FOXK2 and REST (Figure S2). Significantly, analysis of the genomic signatures of FOXK2 and the four corepressor complexes indeed revealed similar binding motifs between FOXK2 and TBL1, FOXK2 and SIN3A, FOXK2 and MTA3, and FOXK2 and REST (Figure 2B). In addition, comparing the characteristic genomic landscapes of TBL1, SIN3A, MTA3, and REST indicate that these proteins were indeed significantly enriched in regions surrounding the FOXK2 binding sites (Figure 2C). Moreover, although overlapping targets did exist, when tag densities from TBL1, SIN3A, MTA3, and REST were clustered against the entire peaks of FOXK2 by seqMINER, an integrated ChIP-seq data interpretation platform (Ye et al., 2011), the tags from the four corepressor complexes were mapped to distinct groups of FOXK2 peaks (Figure 2D), supporting a notion that FOXK2 regulates different sets of genes through interacting with different complexes.

Quantitative ChIP (qChIP) analysis in MCF-7 cells using specific antibodies against FOXK2 on selected genes including *Survivin*, *BCAS3*, *CUL4B*, EZH2, FOXC2, HIF1β, CD44, VEGF, CREBBP, HIG2, and HSP90AA1 showed occupancy of FOXK2 on the promoters of these genes, validating the ChIP-seq results (Figure 3A, upper). Among these genes, *CUL4B*, *VEGF*, and *HIG2* were the co-targets of HDAC3 (NCoR/SMRT complex), *Survivin* and *HIF1β* were co-targeted by SIN3A (SIN3A complex), *BCAS3*, *EZH2*, *FOXC2*, *CD44*, and *CREBBP* were co-regulated by MTA3 (NuRD complex), and *HSP90AA1* was also targeted by CoREST (REST/CoREST complex) (Figure 3A, lower).

To gain further support of the notion that FOXK2 nucleates the four corepressor complexes to regulate distinct target genes, sequential ChIP or ChIP/Re-ChIP experiments were performed on four target genes *VEGF*, *HIF1β*, *EZH2*, and *HSP90AA1*, representing the four corepressor complexes, respectively. In these experiments, soluble chromatins were first immunoprecipitated with antibodies against FOXK2, and the immunoprecipitates were subsequently re-immunoprecipitated with appropriate antibodies. The results showed that, in precipitates, the *VEGF* promoter that was immunoprecipitated with antibodies against FOXK2 could only be re-immunoprecipitated with antibodies against HDAC3 and NCoR, the *HIF1β* promoter could only be re-immunoprecipitated with antibodies against SIN3A and SAP30, the *EZH2* promoter could only be re-immunoprecipitated

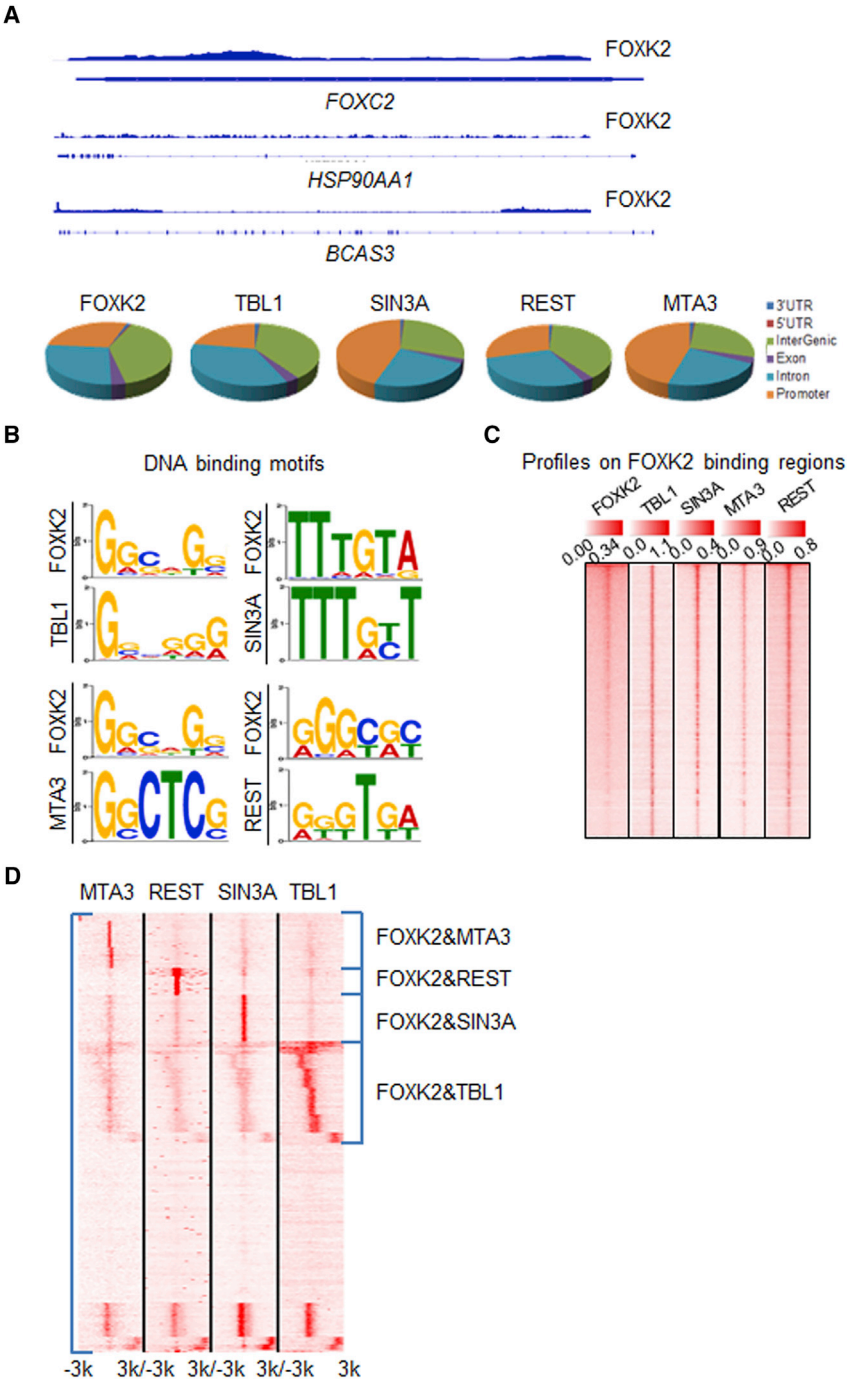

Figure 2. Genome-wide Identification of Transcriptional Targets for FOXK2 and Its Associated Corepressor Complexes

(A) The binding profiles of FOXK2 on representative target genes *FOXC2, HSP90AA1,* and *BCAS3* (upper). ChIPseeker analysis of the genomic distribution of the transcriptional targets of FOXK2 and its associated compressor complexes (lower).

(B) MEME analysis of the DNA-binding motifs of FOXK2, TBL1, SIN3A, MTA3, and REST.

(C) ngs.plot analysis of the density profiles of TBL1, SIN3A, MTA3, and REST on FOXK2 binding sites.

(D) seqMINER clustering of the tag densities of TBL1, SIN3A, MTA3, and REST against the entire peaks of FOXK2 (from −3,000 to +3,000 kb of transcription start sites) using κ-means (linear normalization). Each row of the clustered entities represents the same gene loci.

See also Table S2 and Figure S2.

with antibodies against Mi-2 and MTA3, and the *HSP90AA1* promoter could only be re-immunoprecipitated with antibodies against CtBP1 and CoREST (Figure 3B), strongly supporting the targeting of different genes by FOXK2 and its associated distinct corepressor complexes.

To further validate the ChIP-seq results, FOXK2 was knocked down in MCF-7 cells using three different sets of small interfering RNA and the expression of Survivin, BCAS3, CUL4B, EZH2, FOXC2, HIF1β, CD44, VEGF, CREBBP, HIG2, and HSP90AA1 was analyzed by real-time RT-PCR. The results showed that depletion of FOXK2 resulted in a significant increase, albeit to a different extent, in the expression of all the tested genes (Figure 3C, upper left); whereas HDAC3 knockdown resulted in the increase of the expression of only CUL4B, VEGF, and HIG2, SIN3A knockdown led to elevated expression of only Survivin and HIF1β, MTA3 knockdown affected the expression of only BCAS3, EZH2, FOXC2, CD44, and CREBBP, and CoREST knockdown affected the expression of only HSP90AA1 (Figure 3C, middle left). The knockdown efficiency was verified by real-time RT-PCR (Figure 3C, lower left) and western blotting (Figure 3C, right).

FOXK2 and Its Associated Corepressor Complexes Suppress the Hypoxic Response and Breast Cancer Carcinogenesis

Classification of the transcriptional targets of FOXK2 and its four corepressor complexes using online tool DAVID (https://david.ncifcrf.gov/) with a false discovery rate cutoff value of 0.05 indicate that FOXK2 and its nucleated corepressor complexes regulate several cellular signaling pathways including the cell cycle, DNA damage response, p53 pathway, and hypoxia pathway (Figure S2), which are critically involved in cell proliferation and migration. Particularly, VGFR (Goel and Mercurio, 2013), HIF1β (Semenza, 2012), EZH2 (Chang et al., 2011), HIG2 (Kim et al., 2013; Togashi et al., 2005), CREBBP (Ruas et al., 2002), and HSP90AA1 (Sahu et al., 2012) are all implicated in the hypoxic response, a fundamental feature of solid tumors linked to cell proliferation, survival, angiogenesis, immunosurveillance, metabolism, as well as tumor invasion and metastasis (Gilkes et al., 2014). In addition, other FOXK2 targets including BCAS3

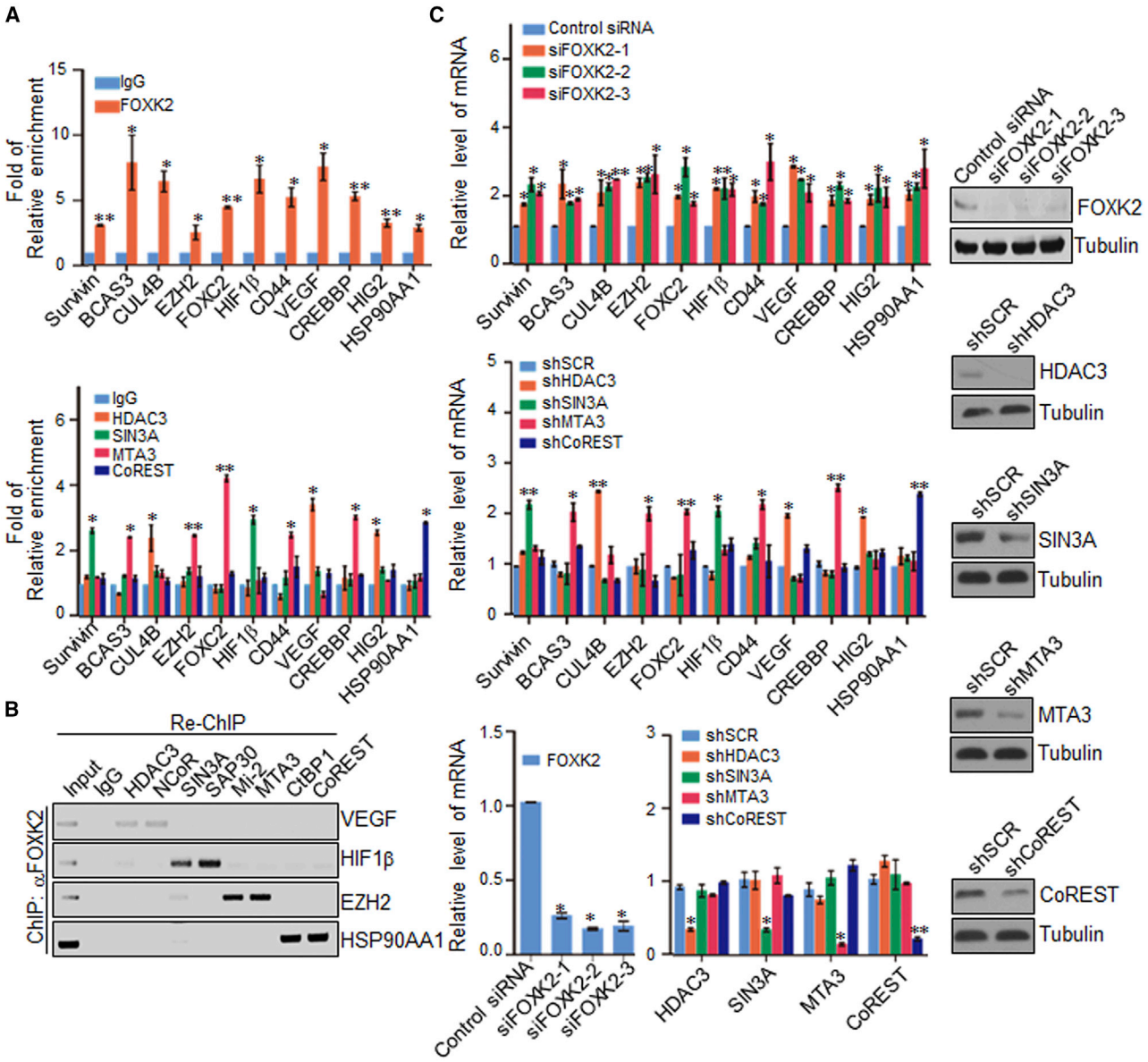

Figure 3. FOXK2-Nucleated Corepressor Complexes Target Distinct Sets of Genes

(A) qChIP verification of the ChIP-seq results on the promoter of the indicated genes with antibodies against the indicated proteins in MCF-7 cells. Results are presented as fold of change over control.

(B) ChIP/Re-ChIP experiments on the promoter of the indicated genes with antibodies against the indicated proteins in MCF-7 cells.

(C) Real-time RT-PCR measurement of the expression of the indicated genes selected from ChIP-seq results in MCF-7 cells under knockdown of FOXK2 with different sets of small interfering RNA (siRNA) or depletion of HDAC3, SIN3A, MTA3, or CoREST using lentivirus-delivered small hairpin RNA (shRNA).

Error bars represent mean ± SD for triplicate experiments (*$p < 0.05$, **$p < 0.01$). The knockdown efficiency was validated by real-time RT-PCR or western blotting.

(Gururaj et al., 2006), FOXC2 (Hollier et al., 2013), and CUL4B (Hu et al., 2012) have been implicated in epithelial-mesenchymal transition (EMT), another hallmark of cancer and an early event in cancer metastasis (Hanahan and Weinberg, 2011).

In order to explore the role of FOXK2 in the development and progression of breast cancer, we first analyzed the effect of loss-of-function of FOXK2 on cell proliferation. Colony formation assays showed that FOXK2 knockdown was associated with a significant increase in colony number of MCF-7 (Figure 4Aa) and T-47D (Figure S3A) cells. Similar results were also obtained in normal human mammary gland epithelial MCF-10A cells (Figure S3B). EdU cell proliferation assays revealed that depletion of FOXK2 in MCF-7 (Figure 4Ab) or in T-47D (Figure S3C) cells was associated with a marked increase in proliferating cells. Growth curve measurement indicates that FOXK2 stable knockdown rendered a much higher growth rate for MCF-7 (Figure 4Ac) and T-47D (Figure S3D) cells. Cell-cycle profiling demonstrated that FOXK2-deficient MCF-7 (Figure 4Ad) and T-47D (Figure S3E) cells exhibited a significant decrease in the percentage of cells in G_0/G_1 phases and an increase in the percentage of cells in S

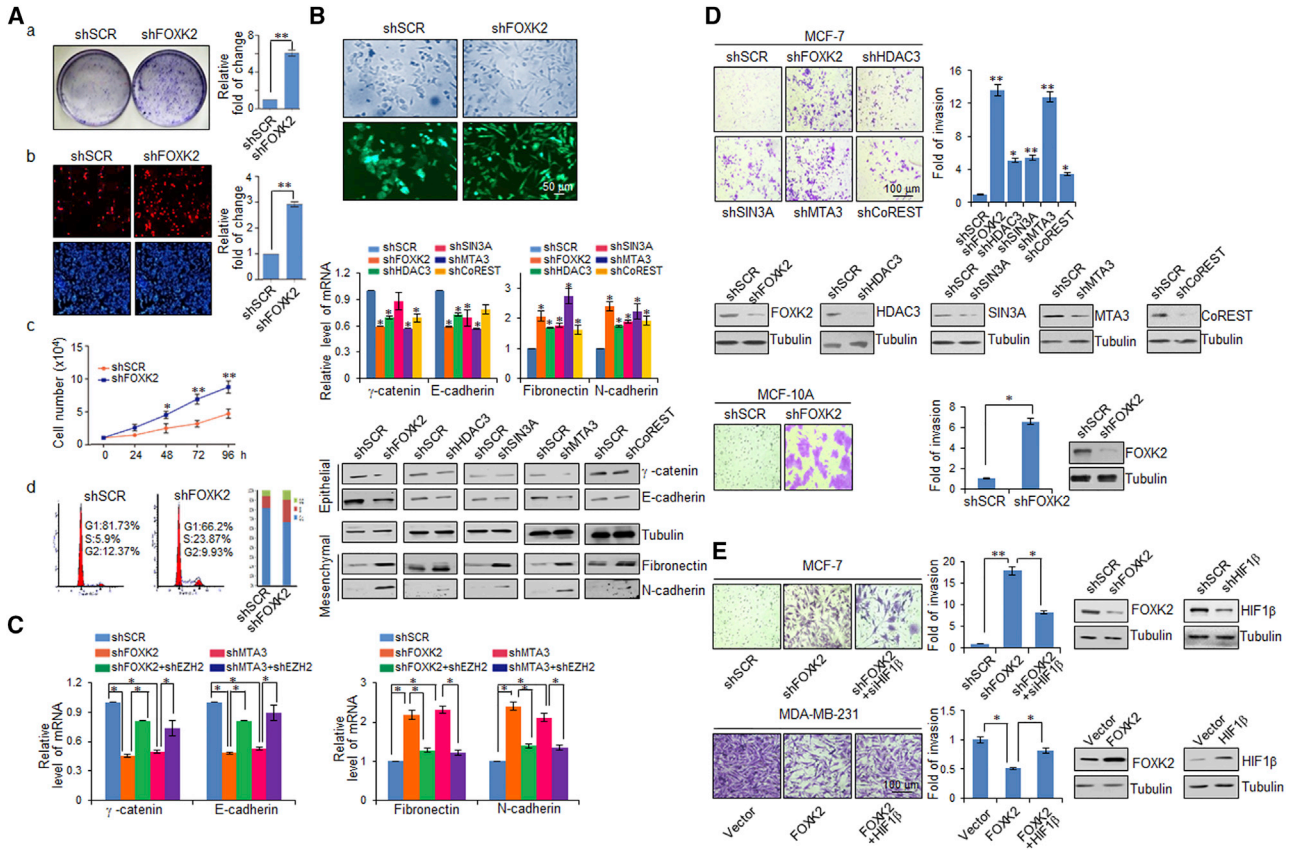

Figure 4. FOXK2 Inhibits Breast Cancer Cell Proliferation and Invasion In Vitro

(A) (a) Colony formation assays in FOXK2-deficient MCF-7 cells. (b) EdU assays in FOXK2-deficient MCF-7 cells. For each group, six different fields were randomly chosen and counted under fluorescent microscopy with 10-fold magnification. Representative images (left) and statistical analysis (right) are shown. (c) Growth curve assays in FOXK2-deficient MCF-7 cells. (d) Flow cytometry of the cell-cycle profile in FOXK2-deficient MCF-7 cells.

(B) FOXK2-deficient MCF-7 cells were imaged by phase-contrast microscopy (upper). The expression of the indicated epithelial or mesenchymal markers was measured in MCF-7 cells upon knockdown of FOXK2, HDAC3, SIN3A, MTA3, or CoREST using lentivirus-delivered shRNA by real-time RT-PCR (middle) or western blotting (lower).

(C) The expression of the indicated epithelial or mesenchymal markers was measured by real-time RT-PCR in synchronized MCF-7 cells infected with lentiviruses carrying shRNA against the indicated targets.

(D) Transwell invasion assays in MCF-7 cells (upper) or MCF-10A cells (lower) infected with lentiviruses carrying shRNA against the indicated targets. Knockdown efficiency was verified by western blotting.

(E) Transwell invasion assays in MCF-7 cells infected with lentiviruses carrying shFOXK2 or shFOXK2 + shHIF1β, or in MDA-MB-231 cells overexpressing FOXK2 or FOXK2 + HIF1β.

Error bars represent mean ± SD for triplicate experiments (*$p < 0.05$, **$p < 0.01$). Knockdown efficiency of was verified by western blotting.

See also Figure S3.

phase. Although, due to massive cell death associated with FOXK2 overexpression, we were unable to perform similar assays with gain-of-function of FOXK2, the above data suggest that FOXK2 is a potent inhibitor of cell proliferation.

Morphologically, while control MCF-7 cells maintained organized cell-cell adhesion and cell polarity, FOXK2-deficient cells exhibited loss of cell-cell contacts, cells became scattered, and the cobble stone-like appearance was replaced by a spindle-like, fibroblastic morphology (Figure 4B, upper), indicative of characteristic morphological changes of EMT. To investigate the potential role of FOXK2 and its associated corepressor complexes in the regulation of EMT, the expression of FOXK2, HDAC3, SIN3A, MTA3, or CoREST was individually knocked down in MCF-7 cells, and the expression of epithelial/mesenchymal markers was analyzed by real-time RT-PCR and western blotting in these cells. The results showed that depletion of FOXK2 or the representative components of its associated corepressor complexes resulted in reduced expression of epithelial markers and more evident induction of mesenchymal markers at both mRNA and protein levels (Figure 4B, lower). Consistent with the observation that EZH2 is targeted and transrepressed by the FOXK2/NuRD (MTA3) complex, knockdown of EZH2 could, at least partially, rescue the changes of EMT markers in FOXK2- or MTA3-deficient cells (Figure 4C). Together, these observations support a role for FOXK2 and its associated corepressor complexes in suppressing EMT.

It is believed that hypoxia and EMT mutually promote each other under malignant conditions (Liu et al., 2015a). In order to

investigate if the regulation of EMT by FOXK2 and its associated corepressor complexes is functionally linked to the HIF1α/HIF1β-directed hypoxia pathway, MCF-7 cell clones with FOXK2, HDAC3, SIN3A, MTA3, or CoREST individually and stably depleted were generated by lentivirus-delivered small hairpin RNA (shRNA) and re-infected with lentiviruses carrying HIF1α shRNA. We found that the alterations of the expression of epithelial and mesenchymal markers associated with depletion of FOXK2, HDAC3, SIN3A, MTA3, or CoREST could be rescued by HIF1α knockdown (Figure S3F, upper). Consistently, digoxin, a cardiac glycoside and well-known inhibitor of HIF1α and HIF2α (Zhang et al., 2008), was able to, at least partially, offset the changes of the expression of EMT markers (Figure S3F, upper).

In order to further support the role of FOXK2 and its nucleated corepressor complexes in the development and progression of breast cancer, we investigated the influence of FOXK2, HDAC3, SIN3A, MTA3, and CoREST on cellular behaviors in breast cancer cells. To this end, the expression of FOXK2, HDAC3, SIN3A, MTA3, or CoREST was individually and stably depleted in MCF-7 cells by lentivirus-delivered shRNA and the invasive potential of these cells was assessed by transwell invasion assays. Consistent with the observations that knockdown of FOXK2, HDAC3, SIN3A, MTA3, or CoREST promoted EMT, we found that loss-of-function of these proteins all led to an increase in the invasive potential of MCF-7 cells (Figure 4D, upper). In agreement, loss of FOXK2 in normal mammary MCF-10A cells was associated with an increased migration of these cells in vitro (Figure 4D lower). Meanwhile, knockdown of HIF1β in FOXK2-depleted MCF-7 cells (with high FOXK2 expression) offset the enhanced cell invasion associated with the loss of FOXK2 (Figure 4E, upper), while forced expression of HIF1β neutralized the inhibited invasion of FOXK2-overexpressing MDA-MB-231 cells (with low FOXK2 expression) (Figure 4E, lower).

To investigate the role of FOXK2 and its associated corepressor complexes in the development and progression of breast cancer in vivo, we first examined the effect of loss-of-function of FOXK2 on the growth/dissemination of tumors developed from breast cancer cells in a mouse model. MDA-MB-231 cells that were engineered to stably express firefly luciferase (MDA-MB-231-Luc-D3H2LN, Xenogen) were infected with lentiviruses carrying control shRNA or FOXK2 shRNA. These cells were then orthotopically implanted onto the abdominal mammary fat pad of 6-week-old immunocompromised severe combined immunodeficiency (SCID) female mice (n = 8). The growth of tumors was monitored weekly by bioluminescence imaging with the IVIS imaging system (Xenogen) over a period of 4 weeks. Tumor metastasis was measured by quantitative bioluminescence imaging after 7 weeks. A metastatic event was defined as any detectable luciferase signal above background and away from the primary tumor site. The results showed that, compared with control, FOXK2 knockdown was associated with not only a significant increase in the growth of the primary MDA-MB-231-Luc-D3H2LN tumors, but also a marked induction of liver and spleen metastasis of the tumors (Figure 5A).

MDA-MB-231 Luc-D3H2LN cells were then infected with lentiviruses carrying shRNA targeting FOXK2, HDAC3, SIN3A, MTA3, CoREST, or FOXK2 + HIF1α. These cells were then injected intravenously into SCID mice (n = 8), and seeding lung metastasis was measured by quantitative bioluminescence imaging after 7 weeks of injection. The results showed that, compared with control, knockdown of FOXK2, HDAC3, SIN3A, MTA3, or CoREST all led to a dramatic increase in lung metastasis of the MDA-MB-231-Luc-D3H2LN tumors (Figure 5B, upper, left). In addition, the effect of FOXK2 depletion on lung metastasis was offset at least partially when HIF1α was simultaneously knocked down (Figure 5B, upper right). The metastases to the lungs were verified by histological staining (Figure 5B, upper right). The efficiency of knockdown was validated by western blotting, and the status of hypoxic response was monitored by measurement of the expression of HIG2 by real-time RT-PCR (Figure 5B, lower). Collectively, these experiments support the notion that FOXK2 recruits multiply corepressor complexes to suppress breast cancer carcinogenesis through targeting the hypoxia pathway.

FOXK2 Is Transactivated by ERα and Transrepressed, via Successive Feedback, by HIF1β and EZH2

Profiling of the expression of FOXK2 and its associated corepressor complexes in breast cancer lines indicates that the protein levels of FOXK2 (Figure 6A, left) and the representative components of its associated corepressor complexes (Figure S4A) are generally higher in ERα$^+$ cell lines than in ERα$^-$ cell lines. In corroboration, analysis of public dataset (GEO: GSE5460) showed that the level of FOXK2 is overall higher in ERα$^+$ breast carcinomas than in ERα$^-$ counterparts, and that in ERα$^+$ breast carcinomas the expression level of FOXK2 is positively correlated with that of ERα (Figure 6A, right). To test the hypothesis that FOXK2 is transcriptionally regulated by ERα, MCF-7 cells were cultured in steroids-depleted and phenol red-free medium for 3 days and treated with 17β-estradiol (E2). Measurement of FOXK2 expression in these cells by real-time RT-PCR and western blotting indicates that both mRNA and protein levels of FOXK2 was strongly induced by E2 (Figure 6B, left). Consistently, knockdown of ERα resulted in a reduction and overexpression of ERα was associated with an elevated expression of FOXK2 in MCF-7 cells (Figure 6B, left). Bioinformatics analysis of *FOXK2* promoter using BIOBASE identified multiple potential ERα binding sites, and the targeting of *FOXK2* by ERα was also described in a recent mapping of the genome-wide ERα binding profile (GSM1831738) (Figure 6B, upper right). qChIP experiments using primers corresponding to four potential ERα binding sites on *FOXK2* promoter indeed detected specific ERα binding at a −1,627 to −1,403 bp region upstream of *FOXK2* transcription start site (Figure 6B, lower right). Together, these experiments indicate that FOXK2 is transactivated by ERα in breast cancer cells.

Given our observation that FOXK2 targets the hypoxic response, it is tempting to speculate that the hypoxic response could influence FOXK2 expression. To test this, MCF-7 cells were treated with $CoCl_2$, a chemical inducer of HIF1α (Piret et al., 2002). Measurement of the expression of FOXK2 in these cells by real-time RT-PCR and western blotting indicates that both mRNA and protein levels of FOXK2 decreased upon treatment with $CoCl_2$ (Figure 6C, upper). Consistently, overexpression of HIF1α in MCF-7 cells led to a decreased expression of FOXK2 (Figure 6C, upper), whereas knockdown of HIF1β or treatment with digoxin resulted in elevated expression of

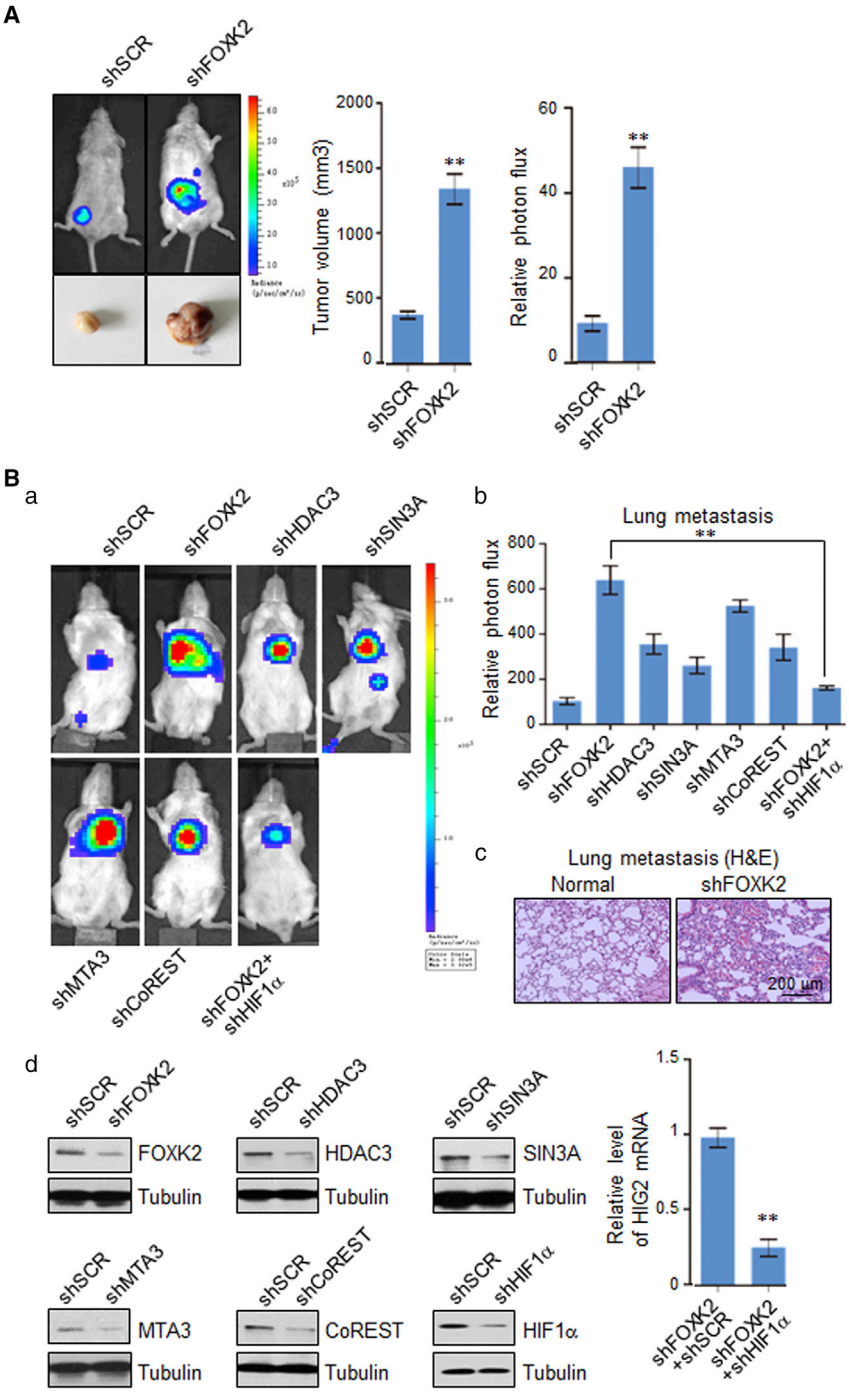

Figure 5. FOXK2 Suppresses the Growth and Metastasis of Breast Cancer In Vivo

(A) MDA-MB-231-Luc-D3H2LN cells infected with lentiviruses carrying either control shRNA (shSCR) or FOXK2 shRNA were inoculated orthotopically onto the abdominal mammary fat pad of 6-week-old female SCID mice (n = 8). Primary tumor size was measured on day 28 and metastases were quantified using bioluminescence imaging after 7 weeks of initial implantation. Representative primary tumors and in vivo bioluminescent images are shown. Error bars represent mean ± SD (**p < 0.01).

(B) (a) MDA-MB-231-Luc-D3H2LN cells infected with lentiviruses carrying shRNA against the indicated targets were injected intravenously through the tail vein of 6-week-old female SCID mice (n = 8). Lung metastasis was monitored by bioluminescent imaging after 7 weeks of injection. Representative in vivo bioluminescent images are shown. (b) Bioluminescent quantitation of lung metastasis. Error bars represent mean ± SD (**p < 0.01). (c) Representative lung metastasis specimens were sectioned and stained with H&E. (d) The knockdown efficiency was verified by western blotting and the expression of HIG2 was measured by real-time RT-PCR as a function of HIF1α knockdown. Error bars represent mean ± SD (**p < 0.01).

FOXK2 in MDA-MB-231 cells (Figure 6C, lower). These results suggest that the hypoxia pathway negatively regulates the expression of FOXK2.

The hypoxic response is believed to be mediated by the HIF1α/HIF1β heterodimer acting to activate transcription (Gilkes et al., 2014). Thus, the negative regulation of FOXK2 expression by HIF1α/HIF1β must be a result of a secondary effect of hypoxic response. Indeed, scanning the *FOXK2* promoter revealed no HIF consensus sequence. However, it is interesting to note that a HIF consensus sequence was found in the promoter of *EZH2* which is transactivated by HIF1α/HIF1β in responding to hypoxia (Chang et al., 2011). In addition, profiling histone methylation marks on the *FOXK2* promoter by qChIP showed that, among the repressive methylation marks that we examined, H3K27me3 is highly enriched at the *FOXK2* promoter (Figure 6D, left). Given that H3K27me3 is a histone modification catalyzed by EZH2 and our observation that FOXK2 and EZH2 are functionally connected, we hypothesized that HIF links EZH2 to regulate FOXK2 expression. To test this, we first examined the occupancy of HIF1α on *EZH2* promoter. qChIP experiments in MCF-7 cells indeed detected the recruitment of HIF1α on *EZH2* promoter in responding to $CoCl_2$ treatment (Figure 6D, right). EZH2 was then overexpressed in MCF-7 cells or knocked down in MDA-MB-231 cells for the measurement of the expression of FOXK2 in these cells by western blotting. The results showed that overexpression of EZH2 resulted in a decreased expression of FOXK2, while depletion of EZH2 led to an increased expression of FOXK2 (Figure 6E, left), suggesting that FOXK2 is transrepressed by EZH2. In support of this inference, qChIP experiments detected the binding of EZH2 on the promoter of *FOXK2* in MCF-7 cells (Figure 6E, right), and western blotting showed that knockdown of EZH2 in MDA-MB-231 cells resulted in an increased expression of FOXK2, even when hypoxic response was activated by $CoCl_2$, whereas EZH2 overexpression in MCF-7 cells was associated with a

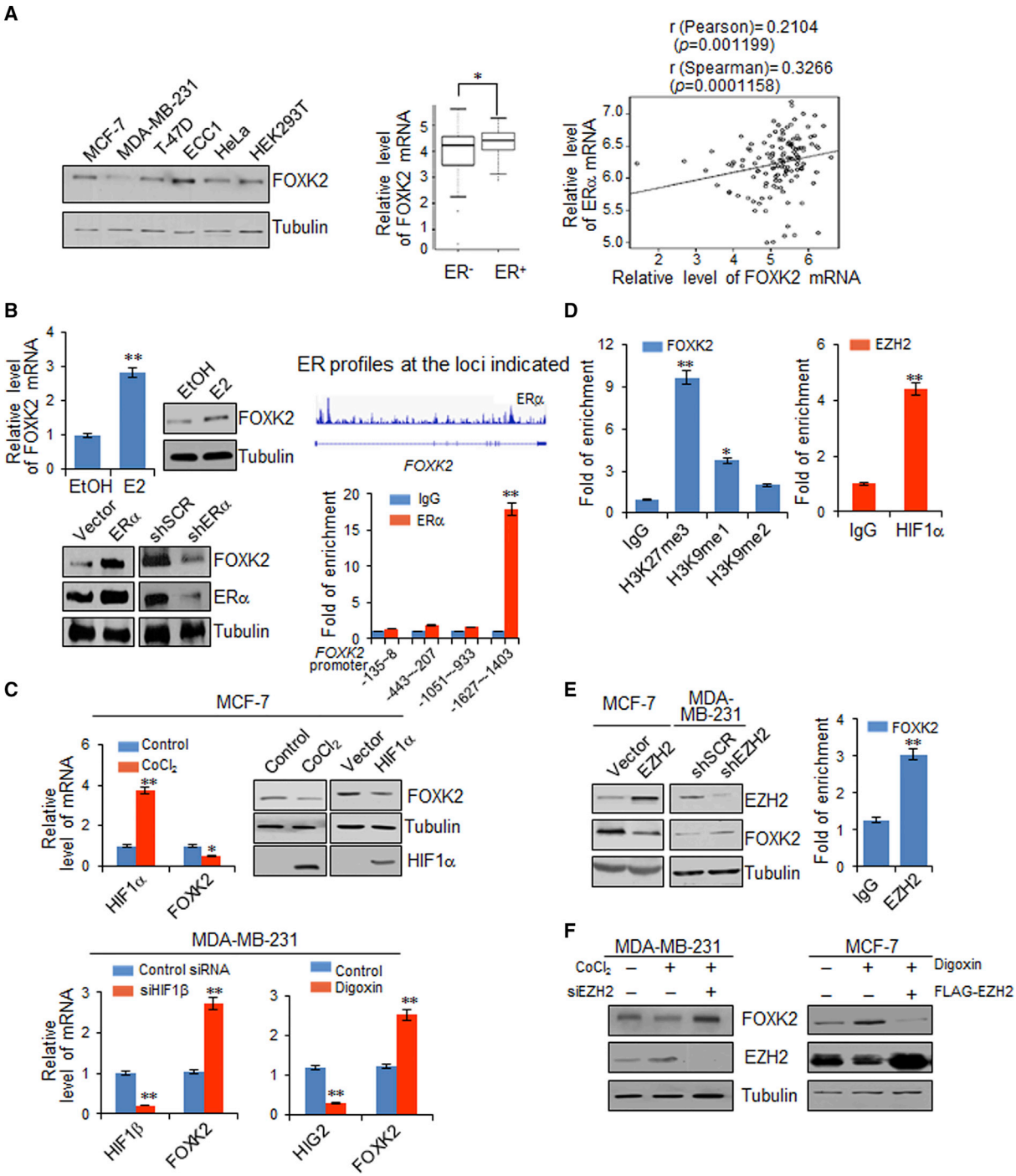

Figure 6. FOXK2 Is Transactivated by ERα and Transrepressed by HIF1β/EZH2

(A) Western blotting analysis of FOXK2 expression in different cancer cell lines (left). Analysis of the public dataset (GEO: GSE5460) for the expression of FOXK2 in ER$^-$ and ER$^+$ breast cancer. The line in the middle, upper, and lower of the boxplot represents the mean, upper, and lower quartile of the relative mRNA level of all samples, respectively (*$p < 0.05$) (middle). Correlation analysis of public dataset (GEO: GSE5460) for the mRNA expression of FOXK2 and ERα by R programming (right).

(B) MCF-7 cells were cultured in steroid-depleted media for 72 hr and treated with E2 for 24 hr prior to the measurement of FOXK2 expression by real-time RT-PCR and western blotting (upper left). ERα was overexpressed or knocked down in MCF-7 cells for the measurement of FOXK2 expression by western blotting (lower left). ERα binding profile on *FOXK2* is shown (upper right). qChIP assays in MCF-7 cells with antibodies against ERα on the predicted sites of *FOXK2* gene promoter (lower right). Error bars represent mean ± SD (**$p < 0.01$).

(legend continued on next page)

reduction of FOXK2 expression, even when hypoxic response was inactivated by digoxin (Figure 6F). These results point to the existence of a reciprocal successive feedback loop between FOXK2 and EZH2/HIF1β in which FOXK2 transrepresses HIF1β and EZH2, and HIF1β, heterodimerized with HIF1α, transactivates EZH2, which, in turn, transrepresses FOXK2.

FOXK2 Is Downregulated in Breast Carcinomas and Its Expression Is Progressively Lost during Breast Cancer Progression

In order to gain further support of the role of FOXK2 in breast cancer development and progression and to extend our observations to a clinicopathologically relevant context, we collected 25 breast carcinoma samples with paired adjacent normal mammary tissues from breast cancer patients and analyzed by real-time RT-PCR the mRNA expression of FOXK2. We found that the mRNA expression of FOXK2 is downregulated in breast carcinomas in 18 of the paired samples (Figure 7A). In addition, consistent with our working model that FOXK2 and its associated corepressor complexes transcriptionally target EZH2 and HIF1β, when the relative expression levels of EZH2 or HIF1β were plotted against that of FOXK2 in the 25 breast carcinoma samples, significant negative correlations were found (Figure 7B).

Next, we examined FOXK2 protein levels by immunohistochemical staining of a human tissue array containing 30 grade II breast carcinoma samples paired with normal mammary tissues as well as tissue arrays including 140 breast carcinoma samples from patients with grade I (28), II (77), or III (35) breast cancer. Analysis using Image-Pro Plus software showed that the expression of FOXK2 is significantly downregulated in breast carcinoma samples (Figure 7C). Remarkably, we found that the level of FOXK2 expression is negatively correlated with the histological grades of the tumors, suggesting that the expression of FOXK2 is progressively lost during breast cancer progression. Interrogation of a public dataset (GEO: GSE5460) also supports the notion that the expression of FOXK2 is downregulated in breast cancer (Figure 7Da) and, interestingly, we found that the level of FOXK2 expression is correlated with poor prognostic molecular signatures when breast carcinoma samples were further stratified into luminal, $ER\alpha^{-}/PR^{-}/Her2^{+}$, and $ER\alpha^{-}/PR^{-}/Her2^{-}$ subtypes (Figure 7Db, left). Further analysis of these data also showed that the level of FOXK2 expression is negatively correlated with the histological grades of breast cancer (Figure 7Db, right), and that, remarkably, low level of FOXK2 expression in breast carcinomas is strongly correlated with the lymph node positivity of the patients (Figure 7Dc). Moreover, querying Lu's breast cancer dataset in Oncomine (https://www.oncomine.org/) revealed that the levels of EZH2 and HIF1β are positively correlated with the histological grades of breast cancer (Figure 7Dd). Together, these results not only fortify our observation that FOXK2 and its associated corepressor complexes transcriptionally target EZH2 and HIF1β, but also support the existence of the reciprocal feedback regulatory loop between FOXK2 and HIF1β/EZH2.

Finally, Kaplan-Meier survival analysis for the expression of FOXK2 and the clinical behaviors of breast cancer with another online tool (http://kmplot.com/analysis/) showed that high a level of FOXK2 ($p = 0.0099$) was associated with a better overall survival in breast cancer patients (Figure 7E, left). Further stratification of patient groups based on the inverse pattern of the expression of FOXK2 and EZH2 improved the predictive capability of FOXK2 (Figure 7E, right). These data are consistent with a role for FOXK2 in suppressing breast cancer development.

DISCUSSION

We report that FOXK2 acts as a transcription repressor. We showed that the transcriptional regulatory activity of FOXK2 is dependent on HDAC activities, and we found that FOXK2 indeed physically interacts with multiple corepressor complexes that all contain HDAC activities. These results are consistent with previous reports (Bowman et al., 2014; Ji et al., 2014; Okino et al., 2015).

The physical association of FOXK2 with multiple transcription corepressor complexes in one cell lineage is surprising and puzzling. One possibility for this is that FOXK2 is able to interact with all of these protein complexes simultaneously (the simultaneous model). An alternative and more convenient explanation is that FOXK2 is associated with a particular corepressor complex under a particular cellular environment (the differential model). Although, due to the limitation of current technologies, the differential model cannot be definitively excluded, at least in our experiments, by detection of the association of FOXK2 with the four corepressor complexes in synchronized cells, the simultaneous model is favored.

The question is: what is the biological significance or evolution advantage for one transcription factor to nucleate multiple corepressor complexes? In this regard, it is worth noting that nuclear receptors also engage in multiple complexes, accounting for the diversity of gene-regulatory networks and heterogeneity of tumors (Cui et al., 2011; Sharma et al., 2006). Analogously, by interacting with multiple corepressor complexes, the genes regulated by FOXK2 expand and the scope and variety of the impact of FOXK2 extend. Perhaps equally important, each cellular signaling pathway is constituted by multiple components/factors. The role of each individual component/factor within the pathway is restricted stoichiometrically. Thus, association with

(C) MCF-7 cells were treated with $CoCl_2$ for the measurement of FOXK2 expression by real-time RT-PCR (upper left). MCF-7 cells were treated with $CoCl_2$ or transfected with HIF1α for the measurement of FOXK2 expression by western blotting (upper right). MDA-MB-231 cells with HIF1β knockdown or digoxin treatment were analyzed for FOXK2 expression by real-time RT-PCR (lower). Error bars represent mean ± SD (*$p < 0.05$, **$p < 0.01$).

(D) qChIP analysis of *FOXK2* promoter using antibodies against H3K27me3, H3K9me1, and H3K9me2 (left). qChIP analysis of the binding of HIF1α on *EZH2* promoter in MCF-7 cells treated with $CoCl_2$ (right). Error bars represent mean ± SD (*$p < 0.05$, **$p < 0.01$).

(E) EZH2 was overexpressed in MCF-7 cells or knocked down in MDA-MB-231 cells, and the expression of FOXK2 was measured by western blotting (left). The binding of EZH2 on *FOXK2* gene promoter was measured by qChIP in MCF-7 cells (right). Error bars represent mean ± SD for triplicate experiments (**$p < 0.01$).

(F) MDA-MB-231 cells with EZH2 knockdown or/and $CoCl_2$ treatment or MCF-7 cells with EZH2 overexpression or/and digoxin treatment were analyzed by western blotting for FOXK2 expression.

See also Figure S4.

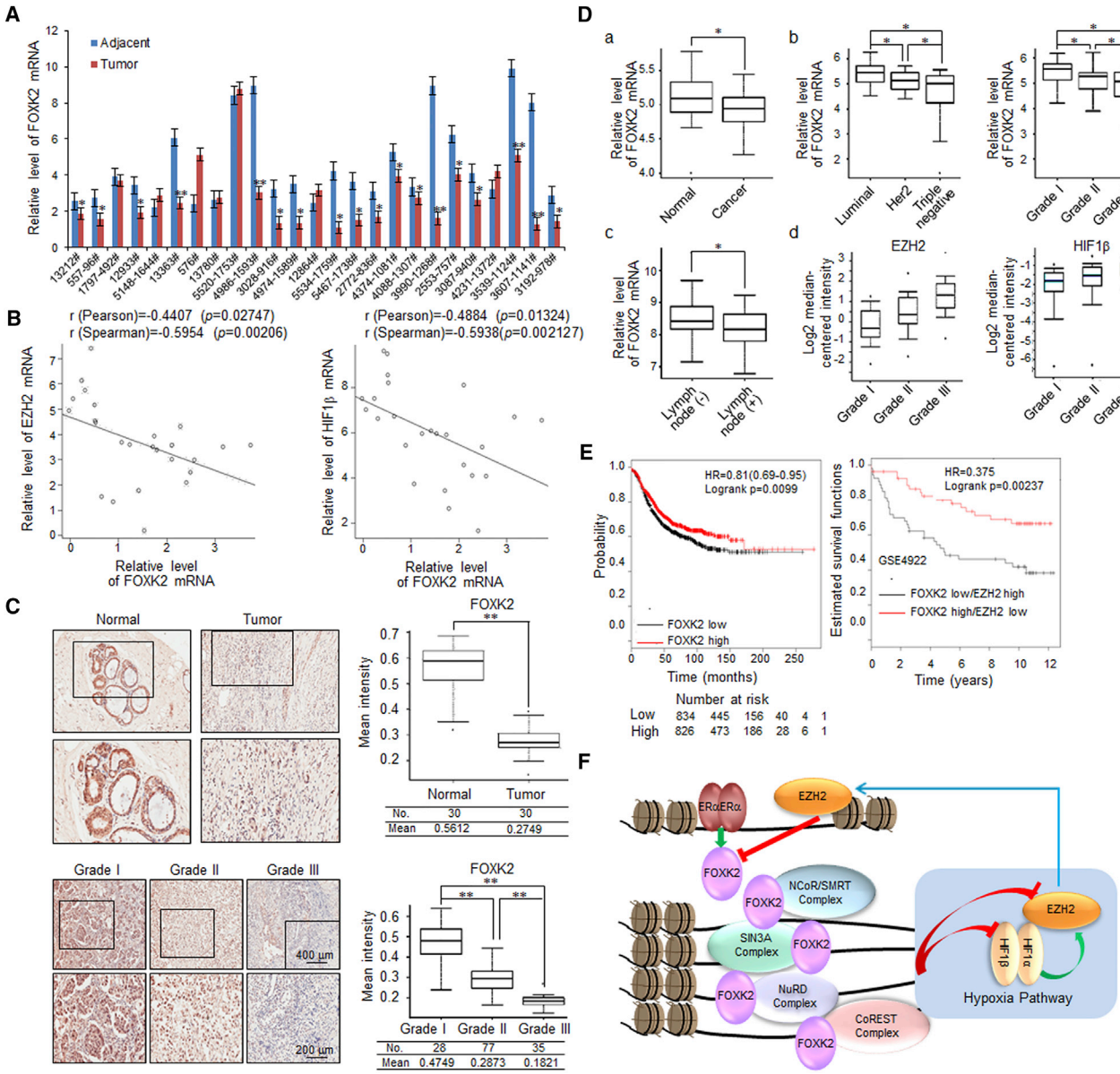

Figure 7. The Expression of FOXK2 Is Progressively Lost during Breast Cancer Progression

(A) Analysis of FOXK2 expression by real-time RT-PCR in 25 breast carcinoma samples paired with adjacent normal mammary tissues. Each bar represents the mean ± SD for triplicate experiments (*$p < 0.05$, **$p < 0.01$).

(B) Analysis of the expression of FOXK2, EZH2, and HIF1β by real-time RT-PCR in 25 breast carcinoma samples. The relative level of FOXK2 was plotted against that of EZH2 or HIF1β. The correlation coefficients were calculated by R programming.

(C) Upper: Immunohistochemical staining of tissue arrays containing 30 grade II breast carcinoma samples paired with adjacent normal mammary tissues for FOXK2 expression. Representative images are shown (left), and the positively stained nuclei were analyzed and the mean staining intensity was calculated using Image-Pro Plus software (right). Lower: Immunohistochemical staining of tissue arrays containing 140 breast carcinoma samples (grades I, II, and III) for FOXK2 expression. Representative images are shown (left), the positively stained nuclei were analyzed and the mean staining intensity was calculated using Image-Pro Plus software (right). The line in the middle, upper, and lower of the boxplot represents the mean, upper, and lower quartile of the relative intensity of FOXK2 staining from all samples, respectively (**$p < 0.01$).

(D) Bioinformatics analysis of the public dataset (GEO: GSE5460) for the expression of FOXK2 in breast carcinoma samples and normal mammary tissues (a). Bioinformatics analysis of the public dataset (GES5460) for the expression of FOXK2 based on the indicated stratifications (b and c). Analysis of Lu's breast cancer dataset (GEO: GSE5460) in Oncomine for the expression of EZH2 and HIF1β based on the indicated stratifications (d) (*$p < 0.05$).

(E) Kaplan-Meier survival analysis of Kaplan-Meier plotter (http://kmplot.com/analysis/) and GEO (GSE4922) for the relationship between survival time of breast cancer patients and their expression of FOXK2 (left) or of FOXK2 and EZH2 (right).

(F) The proposed model for the ERα-FOXK2-HIF1β/EZH2 axis in breast cancer carcinogenesis.

one corepressor complex and regulation of one (or a few) components of a particular cellular signaling pathway may or may not generate an overt and timely effect on the entire pathway, whereas interacting with multiple corepressor complexes and targeting multiple components/factors of a cellular signaling pathway will surely entail more efficient impact on that pathway. In this sense, it is interesting to note that VEGF, HIG2, and CUL4B were targeted by the FOXK2-associated NCoR/SMRT complex; HIF1β and Survivin were regulated by the FOXK2-associated SIN3A complex; CREBBP, EZH2, FOXC2, and BCAS3 were repressed by the FOXK2-associated NuRD complex; and HSP90AA1 was controlled by the FOXK2-associated REST/CoREST complex. As these targets are all functionally linked to the hypoxia pathway, nucleation of the multiple corepressor complexes by FOXK2 and alteration of the expression of these targets would have an imminent and powerful influence on the hypoxia pathway. It is also possible that different corepressor complexes aid or stabilize the binding of FOXK2 to its genomic targets and contribute to the specification of FOXK2 targets. After all, the FOX family proteins are by no means stereotypical transcription factors: for one, a consensus DNA sequence for any class of the FOX family is yet to be determined (Kaestner et al., 2000; Lehmann et al., 2003); and, two, despite their highly conserved sequences, FOX proteins exhibit divergent and even opposing biological activities by either activating or repressing distinct gene networks (Kaestner et al., 2000; Lehmann et al., 2003), and these transcription factors even act non-genomically (Liu et al., 2015b; Wang et al., 2015).

As hypoxia is a fundamental feature of locally advanced solid tumors, the transcriptional repression of the hypoxia pathway by FOXK2 and its associated corepressor complexes is of particular significance, both physiologically and pathologically. During breast cancer progression, lost of FOXK2 will lead to the derepression of the hypoxia signaling, the activation of which promotes EMT and metastasis (Sahlgren et al., 2008; Zhang et al., 2013). Interestingly, our experiments demonstrated that HIF1β is a downstream target of FOXK2, supporting the fluctuation of HIF1β level under hypoxia and its importance in breast cancer progression.

EZH2 is highly expressed in various malignancies including breast cancer, and overexpression of EZH2 is often correlated with advanced stages of cancer progression and poor prognosis (Sauvageau and Sauvageau, 2010). This scenario is consistent with our working model in which the expression of EZH2 is transrepressed by FOXK2. Thus, when the expression of FOXK2 is lost during breast cancer progression, the level of EZH2 is elevated. According to our model, lost expression of FOXK2 leads to the activation of the hypoxia pathway and elevated expression of EZH2, and the hypoxia signaling further augments the level of EZH2, which, in turn, ulteriorly downregulates FOXK2. Apparently, a reciprocal successive feedback loop between FOXK2 and HIF1β/EZH2 exists in breast cancer cells in which FOXK2 represses the hypoxic response and EZH2, which, in turn, relays to downregulate FOXK2 (Figure 7F), further aggravating the situation and promoting breast cancer progression.

Our findings of the regulation of the hypoxia pathway and EZH2 by FOXK2, places FOXK2 in a critical position in controlling breast cancer progression. Consistent with this notion and in agreement with the general belief that patients with ERα$^+$ breast cancer are associated with a better outcome (Liang and Shang, 2013; Shang, 2006), we demonstrated that FOXK2 is positively regulated and transactivated by ERα. Whether or not the lost expression of FOXK2 is due to the lost expression of ERα in breast cancer is currently unknown. At least in our analysis of the clinical samples, the level of FOXK2 is positively correlated with that of ERα. Significantly, our investigation of the TCGA database (Ciriello et al., 2015) found one missense mutation and one frameshift mutation in the *FOXK2* coding sequence. However, the overall frequency of the *FOXK2* mutation appears to be low, and how these mutations might impact on the functionality of FOXK2 and contribute to breast carcinogenesis remain to be investigated.

As stated earlier, although FOXK2 is implicated in severe developmental defects (Hackmann et al., 2013), the precise biological function of FOXK2 is yet to be defined. Perhaps more relevant to our current study, future investigations are needed to delineate the molecular mechanisms, genetic or epigenetic, underlying the lost expression of FOXK2 during the development of breast cancer. In addition, the molecular mechanisms and the evolutionary advantages concerning the association of FOXK2 with multiple corepressor complexes in one cell lineage remain to be investigated. Moreover, although our study focuses on the hypoxia pathway, components of multiple biological signaling pathways including Notch, blood vessel development, and cell metabolism are also identified to be regulated by FOXK2-nucleated protein complexes (Figure S2). Therefore, it is conceivable that FOXK2 orchestrates multiple signaling pathways and controls a batch of biological processes during breast cancer carcinogenesis. Nevertheless, our study demonstrated that FOXK2 is a transcription repressor and a potential tumor suppressor. Our experiments revealed that FOXK2 nucleates multiple corepressor complexes to repress EZH2 and suppress the hypoxia pathway. Our study uncovered a reciprocal successive feedback loop between FOXK2 and HIFβ/EZH2 and an ERα-FOXK2-HIFβ/EZH2 axis in controlling the development and progression of breast cancer, supporting the pursuit of these molecules as targets for breast cancer intervention.

EXPERIMENTAL PROCEDURES

In Vivo Metastasis

MDA-MB-231 cells that had been transfected to stably express firefly luciferase (Xenogen) were infected with lentiviruses carrying control shRNA, shFOXK2, shCoREST, shSIN3A, shHDAC3, shMTA3, or shFOXK2 + shHIF1α. These cells were inoculated into the left abdominal mammary fat pad (3–4 × 10^6 cells) of 6-week-old female SCID mice or injected into the lateral tail vein (1–3 × 10^6 cells) of 6-week-old female SCID mice. For bioluminescence imaging, mice were injected abdominally with 200 mg/g of D-luciferin in PBS. Fifteen minutes after injection, mice were anesthetized and bioluminescence was imaged with a charge-coupled device camera (IVIS; Xenogen). Bioluminescence images were obtained with a 15 cm field of view, binning (resolution) factor of 8, 1/f stop, open filter, and an imaging time of 30 s to 2 min. Bioluminescence from relative optical intensity was defined manually. Photon flux was normalized to background which was defined from a relative optical intensity drawn over a mouse not given an injection of luciferin. Animal handling and procedures were approved by the Tianjin Medical University Institutional Animal Care.

Tissue Specimens

The samples of carcinomas and the adjacent normal tissues were obtained from surgical specimens from patients with breast cancer for whom complete

information on clinicopathological characteristics was available. Samples were frozen in liquid nitrogen immediately after surgical removal and maintained at –80°C until mRNA and protein extraction. Breast tissue arrays were prepared and subjected to immunohistochemistry analysis with standard DAB staining protocols. All studies were approved by the Ethics Committee of the Tianjin Medical University, and informed consent was obtained from all patients.

Statistical Analysis

Results were reported as mean ± SD for triplicate experiments unless otherwise noted. SPSS V.17.0 and two-tailed unpaired t test were used for statistical analysis. The correlation coefficients were calculated by R programming. Breast tumor datasets were downloaded from http://www.ncbi.nlm.nih.gov/geo (Ivhsina; GEO: GSE5460, GES4922, GES1456, GES54275, and GES58812). Data for Kaplan-Meier survival analysis were from http://kmplot.com/analysis/index.php?p=service&cancer=breast.

ACCESSION NUMBERS

ChIP-seq data are deposited at the GEO database (http://www.ncbi.nlm.nih.gov/geo/) with an accession number GEO: GSE84241.

SUPPLEMENTAL INFORMATION

Supplemental Information includes Supplemental Experimental Procedures, four figures, and two tables and can be found with this article online at http://dx.doi.org/10.1016/j.ccell.2016.09.010.

AUTHOR CONTRIBUTIONS

Conceptualization, L.S., Y.W., and Y.S.; Methodology, Lei S., Y.W., Luyang S., C.X., and W.L.; Software, Formal Analysis, and Data Curation, L.S., X.L., and Lei S.; Investigation, L.S., X.Z., Yue W., D.S., Y.H., N.Y., C.Y., B.L., J.G., and Y.D.; Resources, K.C., Luyang S., and J.L.; Writing – Original Draft, L.S. and Y.S.; Writing – Review & Editing, L.S., Lei S., W.L., and Y.S.; Visualization, L.S., X.L., and J.Y.; Funding Acquisition, J.L. and Y.S.

ACKNOWLEDGMENTS

This work was supported by grants (91219201, 81530073, and 81130048 to Y.S.) from the National Natural Science Foundation of China, and a grant (2014CB542004 to J.L.) from the Ministry of Science and Technology of China.

Received: March 9, 2016
Revised: July 8, 2016
Accepted: September 20, 2016
Published: October 20, 2016

REFERENCES

Bowman, C.J., Ayer, D.E., and Dynlacht, B.D. (2014). Foxk proteins repress the initiation of starvation-induced atrophy and autophagy programs. Nat. Cell Biol. *16*, 1202–1214.

Chang, C.J., Yang, J.Y., Xia, W., Chen, C.T., Xie, X., Chao, C.H., Woodward, W.A., Hsu, J.M., Hortobagyi, G.N., and Hung, M.C. (2011). EZH2 promotes expansion of breast tumor initiating cells through activation of RAF1-beta-catenin signaling. Cancer Cell *19*, 86–100.

Ciriello, G., Gatza, M.L., Beck, A.H., Wilkerson, M.D., Rhie, S.K., Pastore, A., Zhang, H., McLellan, M., Yau, C., Kandoth, C., et al. (2015). Comprehensive molecular portraits of invasive lobular breast Cancer. Cell *163*, 506–519.

Cui, S., Kolodziej, K.E., Obara, N., Amaral-Psarris, A., Demmers, J., Shi, L., Engel, J.D., Grosveld, F., Strouboulis, J., and Tanabe, O. (2011). Nuclear receptors TR2 and TR4 recruit multiple epigenetic transcriptional corepressors that associate specifically with the embryonic beta-type globin promoters in differentiated adult erythroid cells. Mol. Cell Biol. *31*, 3298–3311.

Dannenberg, J.H., David, G., Zhong, S., van der Torre, J., Wong, W.H., and Depinho, R.A. (2005). mSin3A corepressor regulates diverse transcriptional networks governing normal and neoplastic growth and survival. Genes Dev. *19*, 1581–1595.

Gilkes, D.M., Semenza, G.L., and Wirtz, D. (2014). Hypoxia and the extracellular matrix: drivers of tumour metastasis. Nat. Rev. Cancer *14*, 430–439.

Goel, H.L., and Mercurio, A.M. (2013). VEGF targets the tumour cell. Nat. Rev. Cancer *13*, 871–882.

Gururaj, A.E., Holm, C., Landberg, G., and Kumar, R. (2006). Breast cancer-amplified sequence 3, a target of metastasis-associated protein 1, contributes to tamoxifen resistance in premenopausal patients with breast cancer. Cell Cycle *5*, 1407–1410.

Hackmann, K., Stadler, A., Schallner, J., Franke, K., Gerlach, E.M., Schrock, E., Rump, A., Fauth, C., Tinschert, S., and Oexle, K. (2013). Severe intellectual disability, West syndrome, Dandy-Walker malformation, and syndactyly in a patient with partial tetrasomy 17q25.3. Am. J. Med. Genet. A *161A*, 3144–3149.

Hanahan, D., and Weinberg, R.A. (2011). Hallmarks of cancer: the next generation. Cell *144*, 646–674.

Hollier, B.G., Tinnirello, A.A., Werden, S.J., Evans, K.W., Taube, J.H., Sarkar, T.R., Sphyris, N., Shariati, M., Kumar, S.V., Battula, V.L., et al. (2013). FOXC2 expression links epithelial-mesenchymal transition and stem cell properties in breast Cancer. Cancer Res. *73*, 1981–1992.

Hu, H.L., Yang, Y., Ji, Q.H., Zhao, W., Jiang, B.C., Liu, R.Q., Yuan, J.P., Liu, Q., Li, X., Zou, Y.X., et al. (2012). CRL4B catalyzes H2AK119 monoubiquitination and coordinates with PRC2 to promote tumorigenesis. Cancer Cell *22*, 781–795.

Ji, Z., Mohammed, H., Webber, A., Ridsdale, J., Han, N., Carroll, J.S., and Sharrocks, A.D. (2014). The forkhead transcription factor FOXK2 acts as a chromatin targeting factor for the BAP1-containing histone deubiquitinase complex. Nucleic Acids Res. *42*, 6232–6242.

Kaestner, K.H., Knochel, W., and Martinez, D.E. (2000). Unified nomenclature for the winged helix/forkhead transcription factors. Genes Dev. *14*, 142–146.

Kim, S.H., Wang, D., Park, Y.Y., Katoh, H., Margalit, O., Sheffer, M., Wu, H., Holla, V.R., Lee, J.S., and DuBois, R.N. (2013). HIG2 promotes colorectal cancer progression via hypoxia-dependent and independent pathways. Cancer Lett. *341*, 159–165.

Lai, A.Y., and Wade, P.A. (2011). Cancer biology and NuRD: a multifaceted chromatin remodelling complex. Nat. Rev. Cancer *11*, 588–596.

Lehmann, O.J., Sowden, J.C., Carlsson, P., Jordan, T., and Bhattacharya, S.S. (2003). Fox's in development and disease. Trends Genet. *19*, 339–344.

Liang, J., and Shang, Y. (2013). Estrogen and cancer. Annual Review of Physiology *75*, 225–240.

Liu, K., Sun, B., Zhao, X., Wang, X., Li, Y., Qiu, Z., Gu, Q., Dong, X., Zhang, Y., Wang, Y., and Zhao, N. (2015a). Hypoxia induced epithelial-mesenchymal transition and vasculogenic mimicry formation by promoting Bcl-2/Twist1 cooperation. Exp. Mol. Pathol. *99*, 383–391.

Liu, Y., Ao, X., Jia, Z., Bai, X.Y., Xu, Z., Hu, G., Jiang, X., Chen, M., and Wu, H. (2015b). FOXK2 transcription factor suppresses ERalpha-positive breast cancer cell growth through down-regulating the stability of ERalpha via mechanism involving BRCA1/BARD1. Sci. Rep. *5*, 8796.

Okino, Y., Machida, Y., Frankland-Searby, S., and Machida, Y.J. (2015). BRCA1-associated protein 1 (BAP1) deubiquitinase antagonizes the ubiquitin-mediated activation of FoxK2 target genes. J. Biol. Chem. *290*, 1580–1591.

Piret, J.P., Mottet, D., Raes, M., and Michiels, C. (2002). CoCl2, a chemical inducer of hypoxia-inducible factor-1, and hypoxia reduce apoptotic cell death in hepatoma cell line HepG2. Ann. N. Y. Acad. Sci. *973*, 443–447.

Ruas, J.L., Poellinger, L., and Pereira, T. (2002). Functional analysis of hypoxia-inducible factor-1 alpha-mediated transactivation. Identification of amino acid residues critical for transcriptional activation and/or interaction with CREB-binding protein. J. Biol. Chem. *277*, 38723–38730.

Sahlgren, C., Gustafsson, M.V., Jin, S., Poellinger, L., and Lendahl, U. (2008). Notch signaling mediates hypoxia-induced tumor cell migration and invasion. Proc. Natl. Acad. Sci. USA *105*, 6392–6397.

Sahu, D., Zhao, Z.W., Tsen, F., Cheng, C.F., Park, R., Situ, A.J., Dai, J.Y., Eginli, A., Shams, S., Chen, M., et al. (2012). A potentially common peptide

target in secreted heat shock protein-90 alpha for hypoxia-inducible factor-1 alpha-positive tumors. Mol. Biol. Cell *23*, 602–613.

Sauvageau, M., and Sauvageau, G. (2010). Polycomb group proteins: multi-faceted regulators of somatic stem cells and cancer. Cell Stem Cell *7*, 299–313.

Semenza, G.L. (2012). Hypoxia-inducible factors in physiology and medicine. Cell *148*, 399–408.

Shang, Y. (2006). Molecular mechanisms of oestrogen and SERMs in endometrial carcinogenesis. Nat. Rev. Cancer *6*, 360–368.

Sharma, D., Saxena, N.K., Davidson, N.E., and Vertino, P.M. (2006). Restoration of tamoxifen sensitivity in estrogen receptor-negative breast cancer cells: tamoxifen-bound reactivated ER recruits distinctive corepressor complexes. Cancer Res. *66*, 6370–6378.

Togashi, A., Katagiri, T., Ashida, S., Fujioka, T., Maruyama, O., Wakumoto, Y., Sakamoto, Y., Fujime, M., Kawachi, Y., Shuin, T., and Nakamura, Y. (2005). Hypoxia-inducible protein 2 (HIG2), a novel diagnostic marker for renal cell carcinoma and potential target for molecular therapy. Cancer Res. *65*, 4817–4826.

Wang, W., Li, X., Lee, M., Jun, S., Aziz, K.E., Feng, L., Tran, M.K., Li, N., McCrea, P.D., Park, J.I., and Chen, J. (2015). FOXKs promote Wnt/beta-catenin signaling by translocating DVL into the nucleus. Dev. Cell *32*, 707–718.

Westbrook, T.F., Martin, E.S., Schlabach, M.R., Leng, Y., Liang, A.C., Feng, B., Zhao, J.J., Roberts, T.M., Mandel, G., Hannon, G.J., et al. (2005). A genetic screen for candidate tumor suppressors identifies REST. Cell *121*, 837–848.

Wong, M.M., Guo, C., and Zhang, J. (2014). Nuclear receptor corepressor complexes in cancer: mechanism, function and regulation. Am. J. Clin. Exp. Urol. *2*, 169–187.

Ye, T., Krebs, A.R., Choukrallah, M.A., Keime, C., Plewniak, F., Davidson, I., and Tora, L. (2011). seqMINER: an integrated ChIP-seq data interpretation platform. Nucleic Acids Res. *39*, e35.

Zhang, H., Qian, D.Z., Tan, Y.S., Lee, K., Gao, P., Ren, Y.R., Rey, S., Hammers, H., Chang, D., Pili, R., et al. (2008). Digoxin and other cardiac glycosides inhibit HIF-1alpha synthesis and block tumor growth. Proc. Natl. Acad. Sci. USA *105*, 19579–19586.

Zhang, L., Huang, G., Li, X., Zhang, Y., Jiang, Y., Shen, J., Liu, J., Wang, Q., Zhu, J., Feng, X., et al. (2013). Hypoxia induces epithelial-mesenchymal transition via activation of SNAI1 by hypoxia-inducible factor -1alpha in hepatocellular carcinoma. BMC Cancer *13*, 108.